MicroRNA-124 inhibits colorectal cancer cell proliferation and suppresses tumor growth by interacting with PLCB1 and regulating Wnt/β-catenin signaling pathway

M.-L. LU¹, Y. ZHANG², J. LI¹, Y. FU¹, W.-H. LI¹, G.-F. ZHAO¹, X.-H. LI¹, L. WEI¹, G.-B. LIU¹, H. HUANG¹

Mingliang Lu and Yu Zhang contributed equally to this work

Abstract. - OBJECTIVE: Colorectal cancer (CRC) is the most common malignancy for cancer-associated death. This study aimed to investigate the effects of microRNA-124 (miR-124) on tumor proliferation of CRC *in vivo* and *in vitro*.

MATERIALS AND METHODS: MiR-124 mimics were synthesized and transfected into SW620 cells, which were divided into SW620, microR-NA-normal control (miR-NC) and miR-124 mimics group. Quantitative Real Time-Polymerase Chain Reaction (qRT-PCR) was used to examine miR-124, chemokine (C-C motif) ligand-20 (CCL20), tankyrase-2 (TNKS2), phospholipase Cbeta1 (PLCB1) and Wnt4. Cell counting kit-8 (CCK-8) was employed to evaluate cell proliferation. The interaction between miR-124 and PLCB1 was tested with the Dual-Luciferase assay. Cell cycle, apoptosis and invasion were also evaluated. CRC xenograft mouse model was established and tumor size was measured. Hematoxylin and eosin (HE) was used to examine inflammation. Western blot was utilized to detect Wnt4.

RESULTS: MiR-124 was over-expressed in SW620 cells, significantly reduced CCL20 and enhanced TNKS2 compared to that of the miR-NC group (p<0.05). MiR-124 might play roles by initiating PLCB1 expression. MiR-124 significantly decreased cell viability compared to the miR-NC group (p<0.05). MiR-124 regulated cell cycle and markedly induced apoptosis and inhibited cell invasion compared to the miR-NC group (p<0.05). MiR-124 significantly decreased tumor size of CRC models compared to miR-NC mice (p<0.05). MiR-124 remarkably alleviated inflammation of tumor tissues. MiR-124 markedly enhanced Wnt4 expression compared to the miR-NC group (p<0.05).

CONCLUSIONS: MiR-124 inhibited tumor cell proliferation *in vitro* and suppressed tumor growth *in vivo* by interacting with PLCB1 and regulating the Wnt/β-catenin signaling pathway.

Key Words

Colorectal cancer, MicroRNA-124, Proliferation, Wnt/Đ-catenin signaling pathway.

Introduction

Colorectal cancer (CRC) is the third leading reason and the most common malignancy for the cancer-associated death in the whole world^{1,2}. In China, CRC has become the fifth cancer-associated death among all malignances³. The incidence of CRC has been increasing year by year and even achieves 1 million new cases per year, with more than 600000 deaths annually^{4,5}.

In recent years, although the radiotherapy, chemotherapy and surgery have been extensively applied for treating CRC and received satisfactory outcomes in early-stage patients, the prognosis of advanced-stage patients is still poor^{2,6}. Meanwhile, the 5-year survival rate and overall survival rate of CRC patients are also poor⁷, due to the metastasis and invasion of tumor cells to the distant tissues, such as liver, lung tissue^{8,9}. Therefore, further investigations for discovering the novel therapeutic targets involved in the pathogenesis and progression of CRC are required urgently. MicroRNAs (miR-NAs) are a series of non-coding RNAs that consist of 18 to 25 nucleotides and could regulate the gene expression by binding to the 3'-untranslated region (3'-UTR) of targeting RNAs¹⁰. Researchers¹¹⁻¹³ reported that several miRNAs

¹Department of Gastroenterology, The Second Affiliated Hospital, Kunming Medical University, Kunming, Yunnan Province, China.

²Department of Gastroenterology, The First People's Hospital of Yunnan Province, Kunming, Yunnan Province, China.

abnormally express in the human cancer cells, such as colon cancer, breast cancer, cervical cancer and gastric cancer, play important roles in tumor cell differentiation, proliferation and cell apoptosis. MicroRNA-124 (miR-124) is considered to be a brain-enriched microRNA and associates with the neural and physiological development¹⁴. MiR-124 plays critical roles in inhibiting tumor growth¹⁵, especially for the brain tumors and the other solid tumors¹⁶. However, the anti-tumor effects of miR-124 on the CRC tumorigenesis have not been fully clarified and the associated mechanisms are also elusive. The phospholipase Cbeta1 (PLCB1) gene is always over-expressed in the hippocampus and cerebral cortex of the brain, and plays an important role in triggering the functional and structural adaptation in critical periods of development in humans¹⁷. Cabana Dominguez et al¹⁸ showed that PLCB1 participates in the drug-resistance or drug-dependence when regulated by the other molecules; therefore, we explored the association of PLCB1 with CRC cells. Song et al19 indicated that many tumors exhibit the dysfunctions of the Wnt/β-catenin signaling pathway. The dysfunction of the Wnt/β-catenin signaling pathway also causes uncontrolled cell differentiation and proliferation. Recently, the Wnt/β-catenin signaling pathway was found to be involved in the proliferation, invasion and metastasis of CRC cells²⁰. Therefore, we investigated the roles of the miR-124 molecule in the pathogenesis of colorectal cancer in this work. Also, the association between miR-124 and PLCB1 gene or Wnt/β-catenin signaling pathway in vivo and in vitro levels were evaluated, respectively.

Materials and Methods

Cell Culture

The human colorectal cancer cell line, SW620, was purchased from the Shanghai Cell Bank of China Academia Sinica (Shanghai, China). The SW620 cells were cultured in L-15 medium (Gibco, Grand Island, NY, USA) supplemented with 10% fetal bovine serum (FBS; Gibco, Grand Island, NY, USA) and 1% penicil-lin-streptomycin (Beyotime Biotech., Shanghai, China) at 37°C in 5% CO₂. The present study was approved by the Ethics Committee of The Second Affiliated Hospital, Kunming Medical University (Kunming, China).

MiR-124 Mimics Synthesis and Trial Grouping

The targeting oligonucleotides for miR-124 were synthesized by Western Biotech. (Chongqing, China) according to the candidate sequence (5'-UAAGGCACG CGGUGAAUGCC-3'). Also, the sham control oligonucleotides for control were also synthesized due to the candidate sequence (5'-CGCTTCUCGUUTTTGCGT GTCUT-3'). Then, SW620 cells were randomly divided into 3 groups, including the blank cell group (SW620 group, treating without microRNAs), SW620 cells transfecting with sham control oligonucleotides group (miR-NC group) and SW620 cells transfecting with targeting oligonucleotides group (miR-124 group). The SW620 cells were transfected with miR-NC or miR-124 using Lipofectamine 2000 reagent (Cat. No. 11668-027, Invitrogen, Carlsbad, CA, USA) according to the instructions of the manufacturer.

Ouantitative Real Time-PCR (qRT-PCR) Assay

Total RNAs in SW620 cells or tumor tissues were extracted using TRIzol reagents (Beyotime Biotech. Shanghai, China) due to the instructions of the manufacturer. Complementary DNAs (cDNAs) were synthesized by using Reverse Transcription Regent (Western Biotech., Chongqing, China) and submitted to the qRT-PCR assay. The Sybr Green I PCR reagents (Western Biotech., Chongqing, China) were used to amplify miR-124, chemokine (C-C motif) ligand 20 (CCL20), tankyrase 2 (TNKS2), PLCB1, Wnt4, U6 and β-actin genes due to the candidate primers (Table I). The thermal cycling (CT) parameters were conducted with the followings: a pre-denaturation step at 94°C for 4 min, following with 35 cycles or 94°C for 20 s, 60°C for 30 s and 72°C for 30 s. The relative expression of the above genes was analyzed with the UVP gel scanning system (Mode: GDS8000, UVP, Sacramento, CA, USA) and calculated using $2^{-\Delta\Delta ct}$ method²¹.

Dual-Luciferase Assay

The direct interaction between miR-124 and PLCB1 gene in 293T cells (Shanghai Cell Bank of China Academia Sinica, Shanghai, China) was evaluated employing the Dual-Luciferase assay. The Luciferase activities were examined at 48 h post the pMIRGLO-PLCB1-WT, pMIR-GLO-PLCB1-Mut and hsa-miR-124 (Invitrogen, Carlsbad, CA, USA) transfection, using the Dual-Luciferase Reporter Assay System (Cat. No. E1910, Promega, Madison, WI, USA) due to man-

Table I. Primers for the qRT-PCR assay.

Genes		Sequences	
miR-124	Forward Reverse	TGCGCGTGAGCAGGCTGGAGAAATTAACCA TAAGGCACGCGGTGRGAGCAGGCTGGAGAA	
U6	Forward Reverse	CTCGCTTCGGCAGCACATA CGCTTCACGAATTTGCGTG	
CCL20	Forward Reverse	TTTGCTCCTGGCTGCTTTG GCCAGCTGCCGTGTGAAG	
TNKS2	Forward Reverse	CACAACCATGCCAATGAACG GTTTTCAGCAAAATAAATGCCAG	
Wnt4	Forward Reverse	GGCGTAGCCTTCTCACAGTCC CTTCCTGCCAGCCTCGTTG	
PLCB1	Forward Reverse	GTTGGCTGGGAACTCGTCTG CACTCTGCGATGGCTTCTATG	
β-actin	Forward Reverse	TGACGTGGACATCCGCAAAG CTGGAAGGTGGACAGCGAGG	

ufacturer's instructions. Meanwhile, the Renilla Luciferase plasmid, pRL-SV40, was used to be an internal control for determining the transfection efficiency. Finally, the fluorescence intensity was detected with a microplate reader (Mode: MCC/340, Thermo Fisher Scientific, Waltham, MA, USA). Meanwhile, the SW620 cells were divided into 4 groups, including the pMIRGLO-PLCB1-WT+miR-NC(WT+NC) group, pMIRGLO-PLCB1-WT+miR-124 mimics (WT+miR-124) group, pMIRGLO-PLCB1- Mut+miR-NC (Mut+NC) group, pMIRGLO-PLCB1-Mut+miR-124 mimics (Mut+miR-124) group.

Cell Counting Kit 8 (CCK-8) Assay

The SW620 cell viabilities after transfecting with miR-NC and miR-124 were evaluated with Cell Counting Kit-8 (Cat. No. 96992, Sigma-Aldrich, St. Louis, MO, USA) according to the instructions of the manufacturer. Exponentially growing SW620 cells (1×10⁵ cells/ml) were seeded into one well of a 96-well cell culture plate (Corning Inc., Corning, NY, USA). Then, the miR-NC and miR-124 were transfected to the SW620 cells for 4 h. The SW620 cells were cultured for 24 h, 48 h, 72 h and 96 h, respectively. For every time point above, the CCK-8 solution (at a final concentration of 10 µl/ml medium) was added to the wells and incubated at 37°C for another 1-4 h. Finally, the cell viabilities of SW620 were detected at a wavelength of 450 nm using a microplate reader (Mode: MCC/340, Thermo Fisher Scientific, Waltham, MA, USA) and represented as the optical density (OD) values.

Flow Cytometry for Evaluating Cell Cycle and Apoptosis

The cell cycles of SW620 were evaluated with BD Pharmingen Cell Cycle Kit (Cat. No. 558662, BD Biosciences, Franklin Lakes, NJ, USA), depending on the instructions of the manufacturer. 25 µl of propidium iodide (PI) was added to SW620 cells to stain DNA in the dark at 37°C. Thirty minutes after the incubation, the stained DNA contents were observed and analyzed with a FACS Vantage SE flow cytometer (BD Biosciences, Franklin Lakes, NJ, USA). The early and late apoptosis in the SW620 cells were evaluated with a BD Pharmingen FITC Annexin V Apoptosis Detection Kit (Cat. No. 556570, BD Biosciences, Franklin Lakes, NJ, USA), due to the instructions of the manufacturer. The early and late apoptotic staining cells were observed and captured with a FACS Vantage SE flow cytometer (BD Biosciences, Franklin Lakes, NJ, USA). The early and late apoptotic rates were also analyzed with the CELIQUEST software (BD Biosciences, Franklin Lakes, NJ, USA). The upper-right quadrant represented the late apoptosis, and the lower right quadrant represented the early apoptosis.

Transwell Assay

250 µl of cell culture medium containing 1×10⁵ SW620 cells was added to the upper chamber of the transwell system (Corning Inc., Corning, NY, USA). The lower chamber of the transwell system was incubated with 200 µl L-15 medium supplementing with 10% FBS (Gibco, Grand Island, NY, USA). The SW620 Cells were permitted to

migrate to the lower chamber of the membrane for 48 h at 37°C. Then, SW620 cells in upper surface were removed and the chambers were fixed with 4% paraformaldehyde (Sigma-Aldrich, St. Louis, MO, USA) for 20 min. The chambers were washed with Phosphate-Buffered Saline (PBS, Beyotime Biotech. Shanghai, China) and stained with 1% (w/v) crystal violet (Sigma-Aldrich, St. Louis, MO, USA) for 5 min. Finally, the numbers of SW620 cells were observed and counted with an inverted microscope (Model: CKX53, OLYM-PUS, Tokyo, Japan).

CRC Xenograft Mouse Model Establishment and Tumor Volume Measurement

The female BALB/c nude mice (weighing from 24±2 g and aging from 4 to 8 weeks) were purchased from Chongqing Tengxin Biotech. Co. Ltd. (Chongqing, China). The animal experiments in this study were approved by the Ethics Committee of The Second Affiliated Hospital, Kunming Medical University, Kunming, China. The BALB/c nude mice were fed with the standard food (CLEA Japan Inc., Tokyo, Japan) and water freely with 12 h/12 h cycle of light/dark at a temperature of 22-25°C. The human SW620 cells (2×10⁶/200 µl) were subcutaneously injected to the flanks of BALB/c nude mice for 8 days. All of the 10 mice were divided into the miR-NC group (n=5) and miR-124 group (n=5). The tumor volume was measured using the vernier calipers daily for 8 days, and was calculated according to the previously described formula²². Finally, the mice were anesthetized by using 3.5% chloral hydrate (at a final concentration of 10 ml/10 g body weight) and sacrificed. The tumor tissues were isolated and fixed with 4% paraformaldehyde (Sigma-Aldrich, St. Louis, MO, USA) at 4°C and stored at -80°C for the following experiments.

Hematoxylin and Eosin (HE) Staining

Tumor tissues were incubated and fixed by using 4% formaldehyde (Sigma-Aldrich, St. Louis, MO, USA) in Phosphate-Buffered Saline (PBS; Sigma-Aldrich, St. Louis, MO, USA). Then, the inflammatory response was evaluated and analyzed using hematoxylin (Nanjing Jiancheng Biotech., Nanjing, China) and eosin (Beyotime Biotech. Shanghai, China) according to the processes of the routine HE-staining method previously reported²³. The HE stained images were captured and observed with an inverted microscope

(Model: CKX53, OLYMPUS, Tokyo, Japan). The magnification of HE-staining images was 400 ×.

Western Blot Assay

The SW620 cells or tumor tissues were lysed or digested with the radioimmunoprecipitation assay (RIPA; Beyotime Biotech. Shanghai, China) and products were centrifuged for 5 min at 12000 r/min and 4°C. The concentrations of the products were detected using the bicinchoninic acid (BCA) Protein Assay Reagent Kit (Cat. No. 23235, Pierce, Waltham, MA, USA). The isolated proteins were separated using the 15% sodium dodecyl sulfate-polyacrylamide gel electrophoresis (SDS-PAGE; Beyotime Biotech. Shanghai, China) and electrotransferred onto the polyvinylidene difluoride membrane (PVDF; Amersham Biosciences, Little Chalfont, Buckinghamshire, UK) using Trans-Blot SD Semi-Dry Electrophoretic Transfer cell (Mode: 170-3940, Bio-Rad Laboratories, Hercules, CA, USA). PVDF membranes were then incubated with rabbit anti-human Wnt4 polyclonal antibody (1: 2000; Cat. No. ab91226, Abcam, Cambridge, MA, USA) and rabbit anti-human glyceraldehyde-3-phosphate dehydrogenase (GAPDH) polyclonal antibody (1: 2000; Cat. No. ab9485, Abcam, Cambridge, MA, USA) at 4°C overnight. Then, PVDF membranes were washed with PBS three times (5 min per time) and treated using the horseradish peroxidase (HRP)-labeled goat anti-rabbit IgG (1: 1000, Cat. No. AQ132P, Sigma-Aldrich, St. Louis, MO, USA) for 2 h at 37°C. Enhanced chemiluminescence reagent (ECL; Beyotime Biotech. Shanghai, China) was employed to treat PVDF membrane for 2 min in the dark and at room temperature. Eventually, the Western blot bands were captured and analyzed using LabworksTM Analysis Software (version: 4.0, Labworks, Upland, CA, USA).

Statistical Analysis

The data were described as mean \pm standard deviation (SD) or percentage (%) in this study. All of the data were analyzed using the SPSS software 20.0 (SPSS Inc., Armonk, NY, USA). The Student's *t*-test was employed to compare the differences between the two groups. The Tukey's post-hoc test was used to validate the analysis of variance (ANOVA) for comparing the differences among multiple groups. The tests or experiments were repeated for at least six times. The statistical significance was defined as p < 0.05.

Results

MiR-124 Was Overexpressed in SW620 Cells

The miR-124 was transfected into the SW620 cells and the gel images illustrated miR-124 band (Figure 1A). The statistical analysis results showed that the miR-124 expression in the miR-124 mimics group was significantly higher compared to that of the SW620 group and the miR-NC group (Figure 2B, p<0.05). Therefore, the miR-124 was successfully expressed in the SW620 cells.

MiR-124 Reduced CCL20 and Enhanced TNKS2 Expression

CCL20 and THKS2 are the potential targeting genes for the anti-tumor drugs in the intervention of CRC^{24,25}; therefore, both of these molecules were examined in SW620 cells. The results indicated that miR-124 treatment significantly reduced the CCL20 expression in SW620

cells compared to that of the SW620 group and miR-NC group (Figure 1C, p<0.05). Meanwhile, miR-124 markedly enhanced the expression of TNKS2 compared to that of the SW620 group and miR-NC group (Figure 1D, p<0.05).

MiR-124 Played Roles by Initiating PLCB1 Gene Expression

According to the gene information of PLCB2 and miR-124 in the gene bank, the interactive sites were pointed out in this study (Figure 2A). The plasmids containing wide-type PLCB1 gene and mutant PLCB1 gene were synthesized as the sequences in Figure 2B. The agarose gel image of enzyme digestion exhibited the clear PLCB1-WT and PLCB1-Mut bands with appropriate length (Figure 2C). The Dual-Luciferase assay results showed that co-transfection with PLCB1-WT plasmid significantly decreased the relative Luciferase activity in miR-124 expressed SW620 cells (WT+miR-124 group), compared to that of no miR-124 expressed SW620 cells (WT-

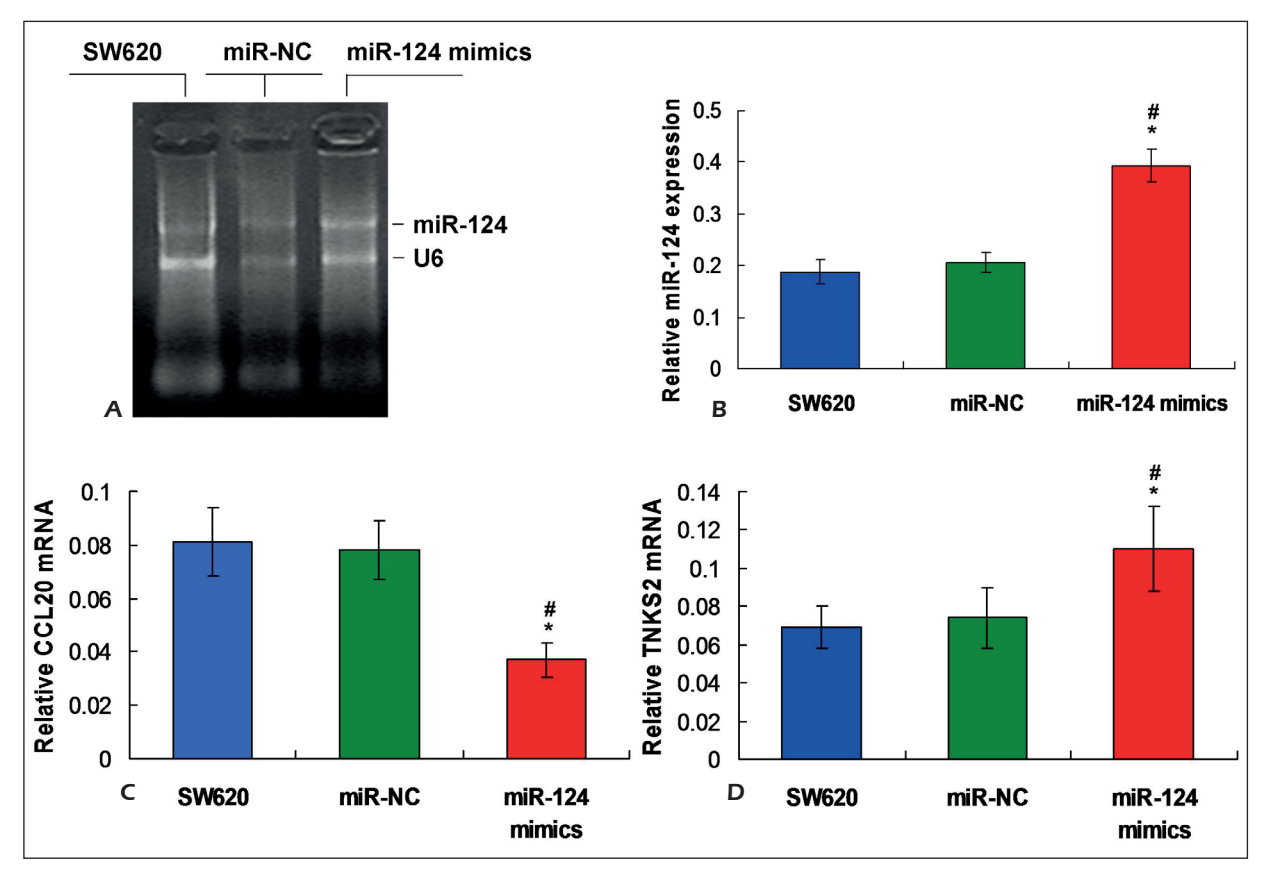


Figure 1. Evaluation for the miR-124 over-expression and associated molecules in SW620 cells. **A**, Gel images for illustrating miR-124 mRNA band. **B**, Statistical analysis for the miR-124 mRNA expression. **C**, Effects of miR-124 over-expression on CCL20 mRNA expression. **D**, Effects of miR-124 over-expression on TNKS2 mRNA expression. *p<0.05 vs. miR-NC group, *p<0.05 vs. SW620 group.

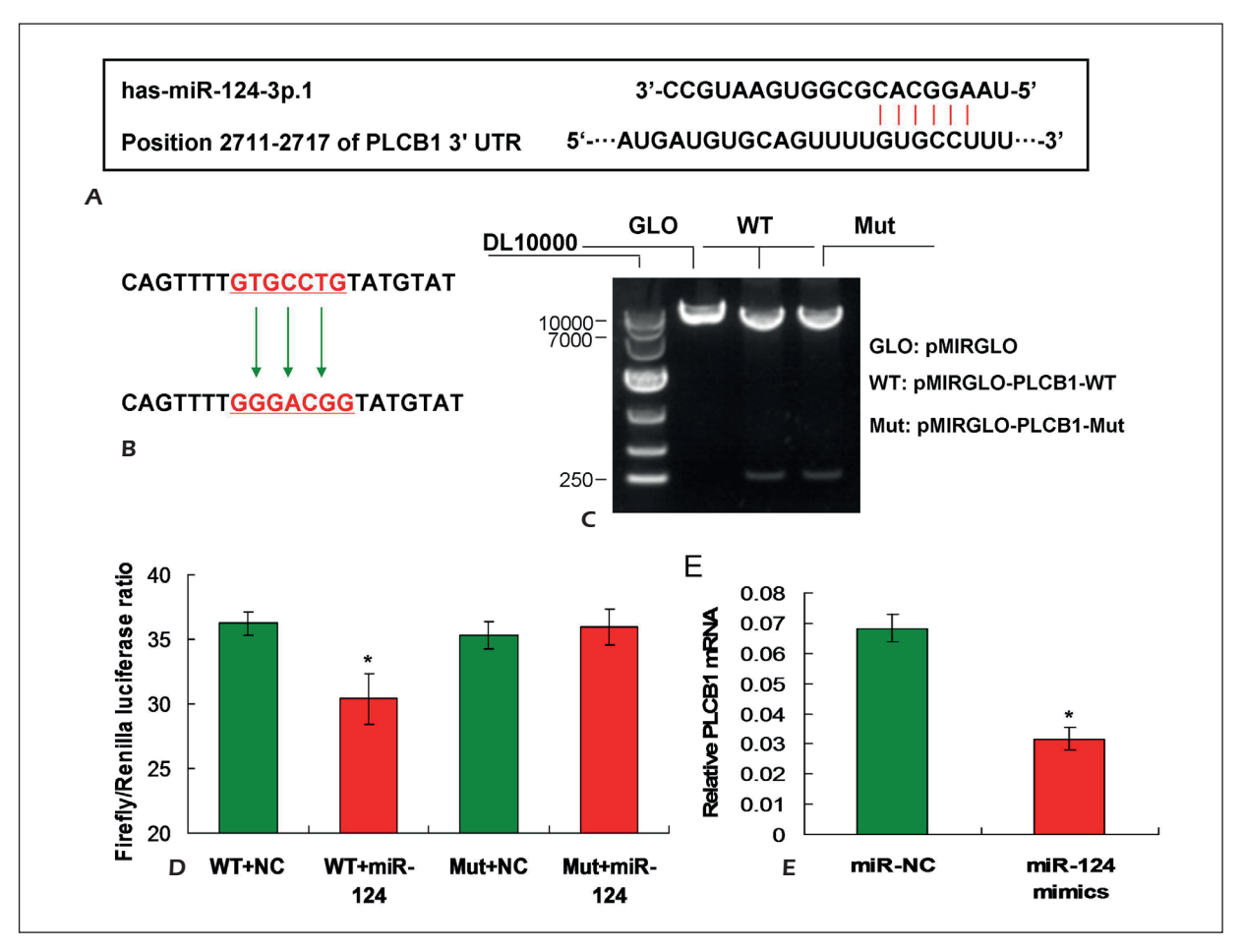


Figure 2. Evaluation for the interaction between miR-124 and PLCB1 gene in SW620 cells. **A**, The interactive sites for miR-124 and PLCB1 gene. **B**, The plasmids containing wide-type PLCB1 gene and mutant PLCB1 gene. **C**, Agarose gel image for the enzyme digestion of PLCB1-WT and PLCB1-Mut bands. **D**, Relative Luciferase activity analysis for miR-124 and PLCB1 gene. **E**, qRT-PCR results for the PLCB1 expression in SW620 cells undergoing miR-124 treatment. *p<0.05 vs. miR-NC group.

NC group) (Figure 2D, p<0.05,). However, when co-transfected with PLCB1-Mut plasmid, there were no significant differences for the relative Luciferase activity between the Mut+miR-124 group and Mut+miR-NC group (Figure 2D, p>0.05). Moreover, the qRT-PCR results indicated that the PLCB1 expression was markedly decreased in the miR-124 mimic group compared to that of the miR-NC group (Figure 2E, p<0.05).

MiR-124 Decreased the SW620 Cell Viability

To evaluate the effects of miR-124 mimic treatment on the SW620 cell viability, the CCK-8 assay was conducted. The results indicated that miR-124 remarkably decreased the SW620 cell viability compared to that of the SW620 group

and miR-NC group, at 48 h, 72 h and 96 h post miR-124 mimics treatment, respectively (Figure 3, p<0.05).

MiR-124 Regulated Cell Cycle and Induced the Apoptosis of SW620 Cells

The cell cycle results indicated that the S-phase cells in the miR-124 mimic group were markedly decreased, and G1/G2-phase cells were significantly increased, compared to that of the SW620 group and miR-NC group (Figure 4, p<0.05). Meanwhile, the flow cytometry assay (Figure 5A) was conducted to examine the early and late apoptosis of SW620 cells. The results indicated that both of the early and late apoptosis cells in the miR-124 mimic group were more compared to that of the SW620 group and miR-NC group (Figure 5B, p<0.05).

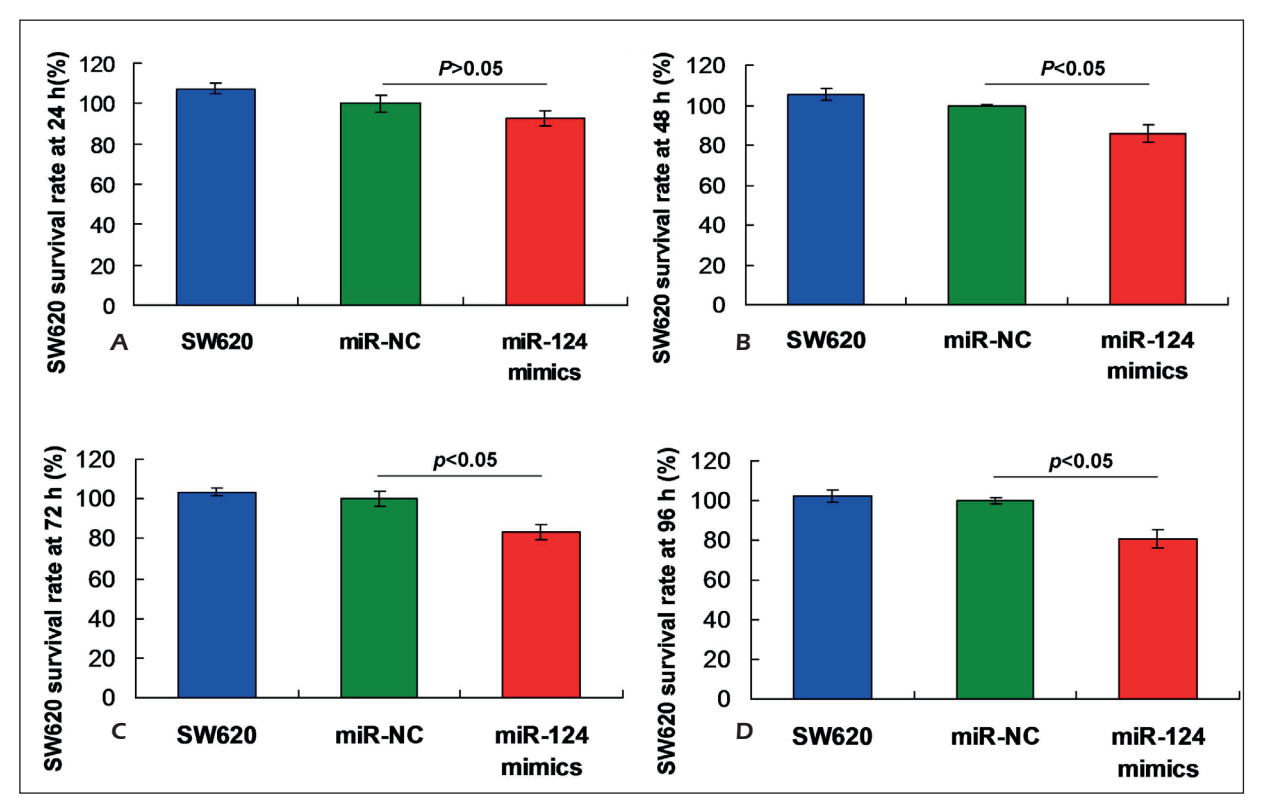


Figure 3. CCK-8 assay for detecting SW620 cell proliferation. **A**, SW620 cell proliferation at 24 h post miR-124 treatment. **B**, SW620 cell proliferation at 48 h post miR-124 treatment. **C**, SW620 cell proliferation at 72 h post miR-124 treatment. **D**, SW620 cell proliferation at 96 h post miR-124 treatment. The p-values were illustrated in the images.

MiR-124 Inhibited SW620 Cell Invasion

To evaluate the invasive viability of the miR-124 transfected SW620 cells, the transwell assay was performed in this work (Figure 6A). The results exhibited that the invasive cells in the miR-124 mimic group were significantly more compared to that of the SW620 group and miR-NC group (Figure 6B, p<0.05).

MiR-124 Decreased the Tumor Volume of CRC Xenograft Mouse Models

In this study, the CRC xenograft mouse models were established and the tumor volumes were examined. Figure 7A showed that the tumors in the miR-124 mimic group were markedly smaller compared to that of the miR-NC group, both due to the *in vivo* tumors and isolated tumors. The statistical analysis results also illustrated that the volume of tumors was significantly smaller in the miR-124 mimics group compared to that of the miR-NC group (Figure 7B, *p*<0.05) at 6 days, 7 days and 8 days post the miR-124 mimic treatments.

MiR-124 Alleviated the Inflammatory Response of Tumor Tissues

To evaluate if the effects of miR-124 mimics treatment on the tumor growth caused inflammation of SW620 cells, the HE staining (Figure 8A) was performed. The results showed that the inflammatory response cells in the miR-124 mimic group were significantly more compared to that of the miR-NC group (Figure 8B, p<0.05).

MiR-124 Activated the Wnt/β-Catenin Signaling Pathway

The previous study reported that microRNA molecules are associated with the Wnt/β-catenin signaling pathway. Therefore, a Wnt/β-catenin key molecule, Wnt4²⁶, was examined in this study. The qRT-PCR assay results indicated that the Wnt4 mRNA levels were significantly higher in miR-124 mimic group compared to that of the miR-NC group (Figure 9A, p<0.01). Furthermore, the Western blot assay results showed that the Wnt4 protein levels were significantly higher in the miR-124 mimic group compared to that of the miR-NC group (Figure 9B, p<0.01).

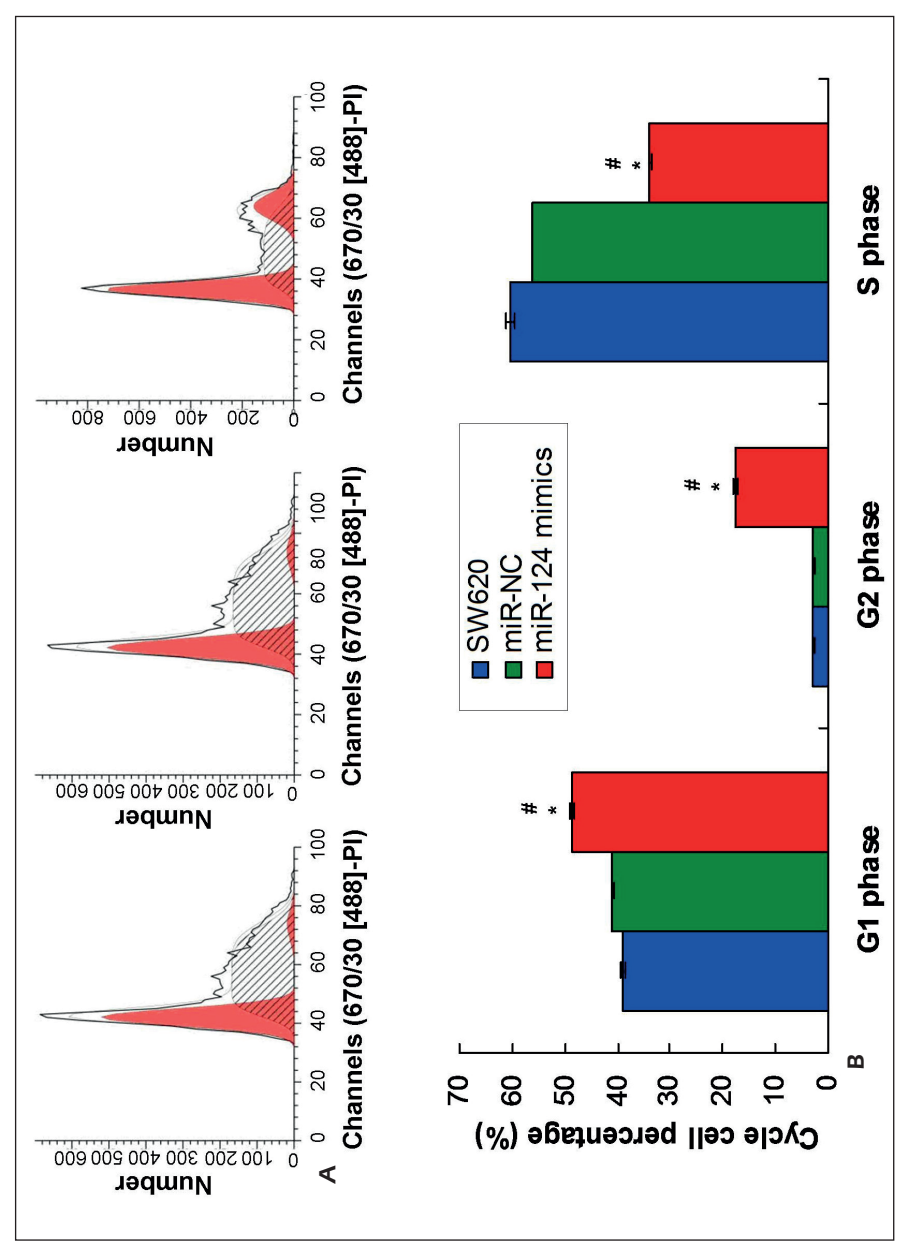


Figure 4. Effects of miR-124 on cell cycle of SW620 cells. **A**, Images for the cell cycle analysis. **B**, Statistical analysis for the cell cycle analysis. *p<0.05 vs. miR-NC group, *p<0.05 vs. SW620 group.

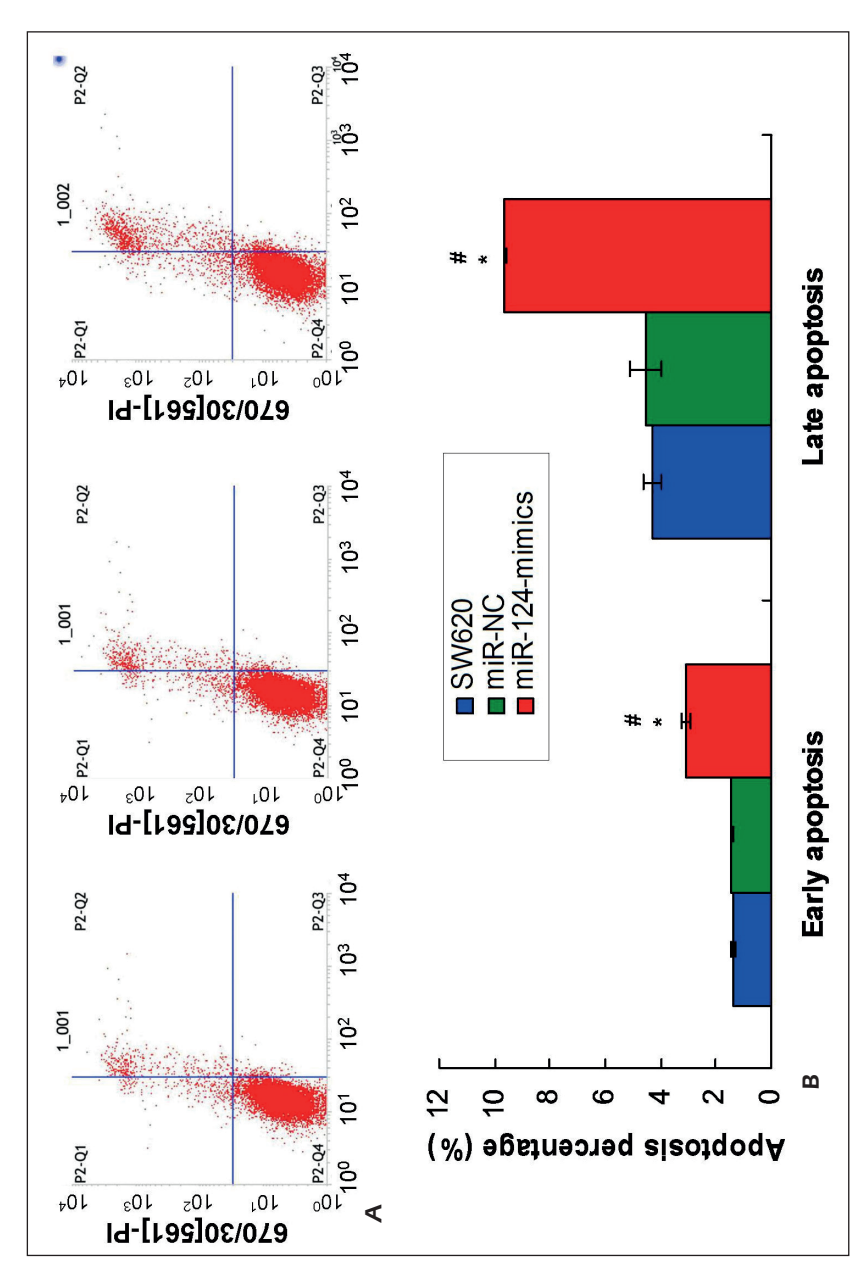


Figure 5. Effects of miR-124 on early apoptosis and late apoptosis of SW620 cells. **A**, Images for the flow cytometry analysis. **B**, Statistical analysis for the early apoptosis and late apoptosis analysis. *p<0.05 vs. miR-NC group, *p<0.05 vs. SW620 group.

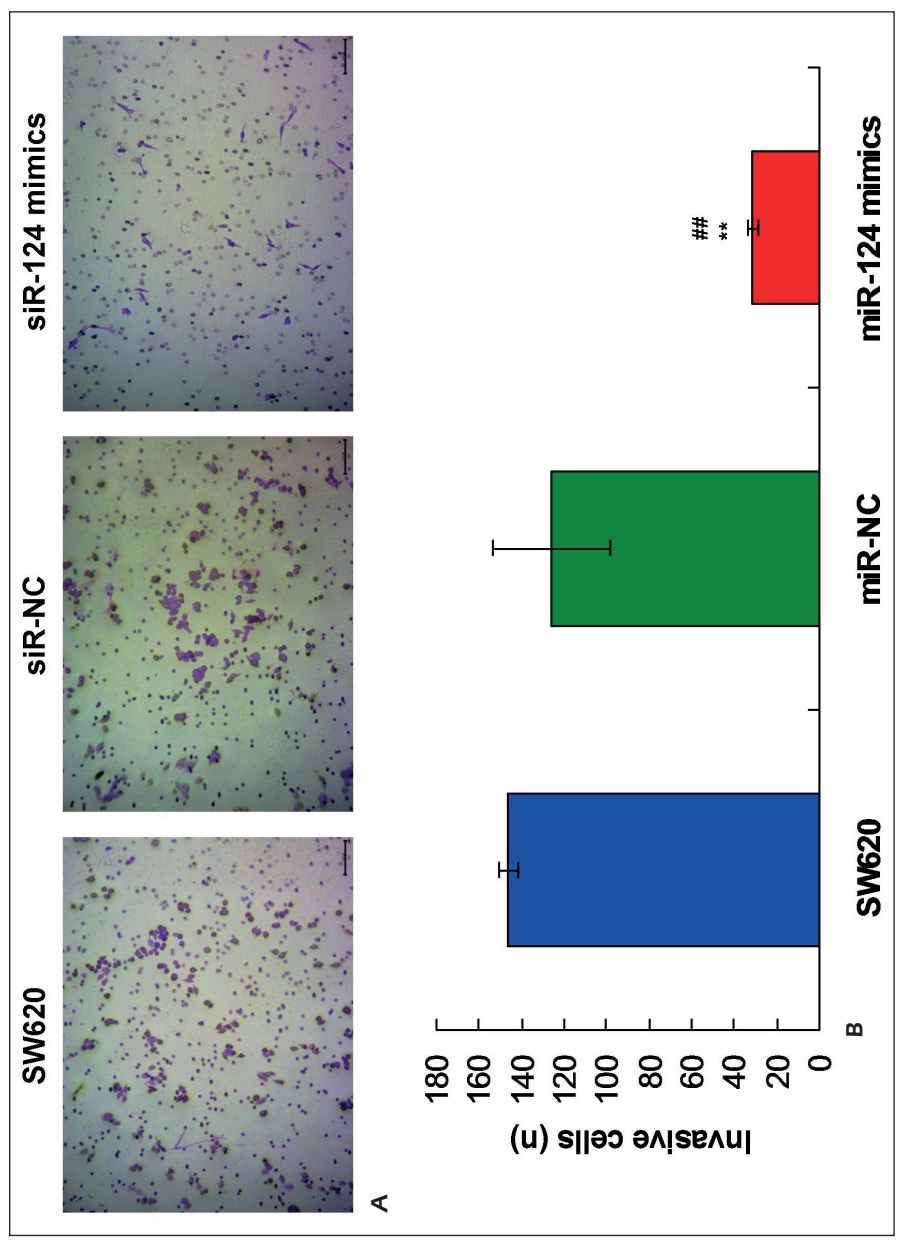


Figure 6. Invasion of the SW620 cells undergoing miR-124 treatment. **A**, Invasive images for the SW620 cells undergoing miR-124 treatment. **B**, Statistical analysis for invasive SW620 cells. **p<0.01 vs. miR-NC group, **p<0.01 vs. SW620 group.

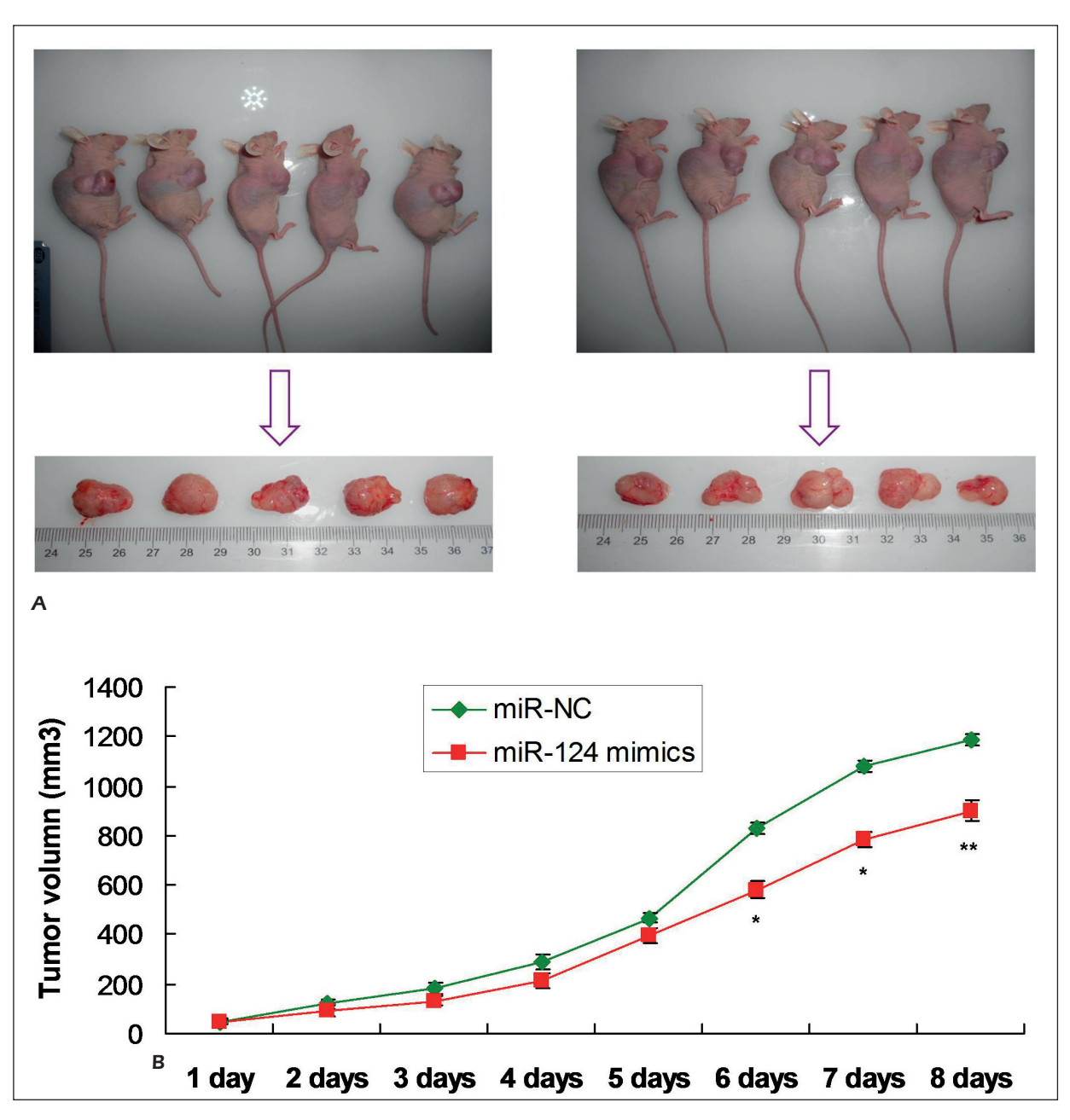


Figure 7. miR-124 decreased tumor size of CRC xenograft mouse models. **A**, Images for tumors in mouse model bodies or isolated tumors. **B**, Statistical analysis for the tumor volume of the isolated tumors. *p<0.05, **p<0.01 vs. miR-NC group.

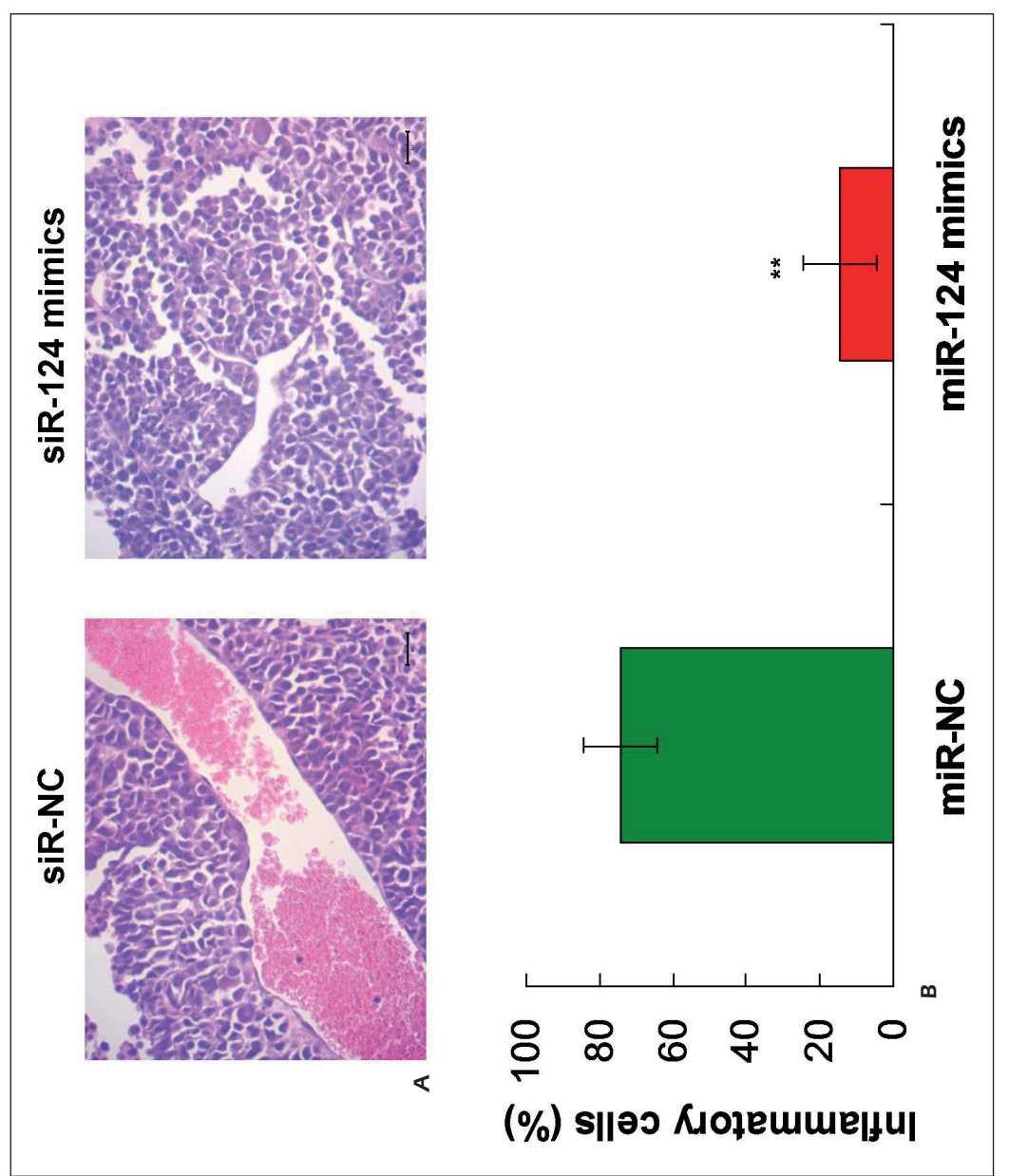


Figure 8. Inflammation of tumor tissues by examining with HE staining. **A**, HE staining images of miR-124 and miR-NC group. **B**, Statistical analysis for the HE staining tumor tissues. **p<0.01 vs. miR-NC group.

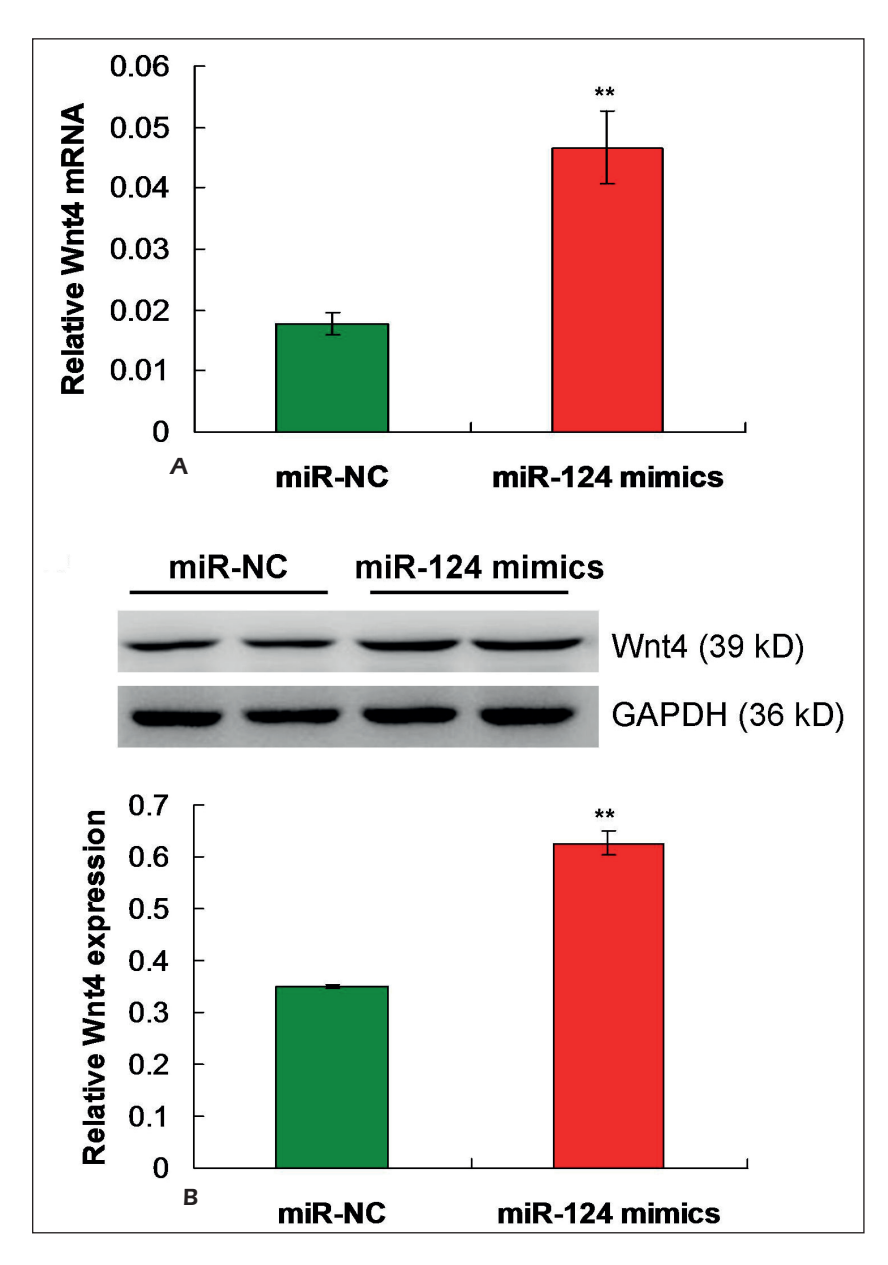


Figure 9. Wnt4 expression evaluation determining by qRT-PCR and Western blot assay. **A**, qRT-PCR assay for detecting the Wnt4 mRNA expression. **B**, Western blot images and statistical analysis for Wnt4 expression. **p<0.01 vs. miR-NC group.

Discussion

Till now, plenty of CRC-specific microRNAs have been discovered for predicting or targeting the cancer cells; the potential mechanism for progression and development in CRC cells has not been fully clarified^{27,28}. Many studies have reported that the miR-124 is down-regulated and plays critical roles in the proliferation, differentiation and metastasis of lung cancer, breast cancer and esophageal cancer²⁹⁻³¹. In the present work, the miR-124 mimics treatment significantly decreased SW620 cell viability, induced apoptosis and inhibited cell invasion in vitro levels. In the CRC xenograft mouse models, the miR-124 mimic treatment also significantly suppressed the tumor formation in vivo levels. All of the above findings suggest that the over-expression of miR-124 is associated with the proliferation and invasion of CRC. We first transfected the miR-124 mimics into the SW620 cells and observed the biological effects of the over-expression of miR-124 on the SW620 cell viability. The in vitro results showed that miR-124 over-expression significantly inhibited the SW620 cell proliferation. Meanwhile, the drug-sensitivity associated molecules, such as CCL20 and THKS224,25, were also examined in vitro level. The qRT-PCR results indicated that the miR-124 markedly down-regulated CCL20 and up-regulated THKS2 expression, which corroborates the findings from the previous study³². These results suggest that miR-124 may participate in the drug-resistance processes in chemotherapy; however, the associated mechanism also needs to be further investigated. The previous study reported that the microRNAs could target the PLCB1 gene³³, which is always over-expressed in the tumor tissues³⁴. Therefore, we discovered the interactive sites of PLCB1 gene binding to the miR-124 gene and synthesized the wide-type PLCB1 gene and mutant PLCB1 gene plasmids. Dual-Luciferase assay results showed that the miR-124 could interact with the wide-type PLCB1 gene, but could not with the Mutant type PLCB1 gene. Moreover, gRT-PCR results showed that miR-124 treatment significantly down-regulated the PLCB1 expression in vitro. These results suggest that miR-124 may regulate the CRC cell line SW620 cell proliferation by down-regulating the expression of PLCB1 gene. We speculated that the down-regulated PLCB1 expression may further decrease the drug-resistance of tumor cells in the chemotherapy, which is needed to be proven in the following study. To explore the reasons that induce the death of SW620 cells, the cell cycle and cell apoptosis were evaluated³⁵. The

results showed that S-phase cells in the miR-124 mimic group were significantly decreased, and G1/ G2-phase cells were markedly increased, compared to that of the SW620 group and miR-NC group. Therefore, the cell cycle assay results exhibited the G1 cell cycle arrest in the miR-124 mimics treated SW620 cells. Moreover, the flow cytometry results also indicated that both the early and late apoptosis cells in the miR-124 mimic group were more compared to that of the SW620 group and miR-NC group. All of the above findings suggest that miR-124 mimics induced the apoptosis by triggering the G1 cell cycle arrest. In our work, we also found that SW620 cell transfected with miR-124 inhibited the invasion-related processes, which is consistent with the previous studies^{6,36}. In this paper, the CRC xenograft mouse models were also successfully established by transplanting the SW620 cells into the mice. The results showed that the miR-124 mimics treatment significantly decreased the tumor sizes compared to the miR-NC group, in both in vivo tumors and isolated tumors. The previous study³⁷ also reported that the miR-124 mimics effectively inhibited the tumor growth in the xenograft breast cancer models, which is consistent with the present work. The HE staining results also illustrated that miR-124 mimics significantly alleviated the inflammatory response compared to that of the miR-NC group, which suggests that decreased tumor size may be associated with the inflammation in the CRC xenograft mouse models. To clarify the mechanism that causes the miR-124 triggered a decrease of tumor sizes, the level of the key molecule of the Wnt/β-catenin signaling pathway, Wnt426, in tumor tissues was evaluated in this work. Both the qRT-PCR assay and Western blot assay indicated that Wnt4 mRNA and protein levels were significantly higher in the miR-124 mimic group compared to that of the miR-NC group. Scholars^{38,39} have also demonstrated the correlation between miR-124 and molecules in the Wnt/β-catenin signaling pathway in a few tumors. Therefore, these results suggest that miR-124 inhibits the tumor cell proliferation in vitro and suppresses tumor growth in vivo, by regulating the Wnt4 molecule of the Wnt/β-catenin signaling pathway.

Conclusions

We found that the SW620 cells transfected with miR-124 demonstrated decreased cell proliferation and invasive viability, and enhanced apoptosis. The interaction between miR-124 and PLCB1

gene might be associated with the drug-sensitivity to tumor cells in chemotherapy. Meanwhile, miR-124 inhibited tumor growth *in vivo* by regulating the Wnt/ β -catenin signaling pathway. The present study suggests that the over-expression of miR-124 provides a potential strategy to inhibit the tumor proliferation *in vitro* and suppress tumor growth *in vivo*. From the clinical viewpoint, the up-regulation of miR-124 might be considered to be a promising therapeutic strategy for CRC progression.

Conflict of Interests

The authors declare that they have no conflict of interest.

References

- FISICHELLA R, CAPPELLANI A, BERRETTA S. MiR-431 inhibits colorectal cancer cell invasion via repressing CUL4B. Eur Rev Med Pharmacol Sci 2018; 22: 5051-5052.
- JEMAL A, BRAY F, CENTER MM, FERLAY J, WARD E, FORMAN D. Global cancer statistics. CA Cancer J Clin 2011: 61: 69-90.
- 3) Herszenyi L, Tulassay Z. Epidemiology of gastrointestinal and liver tumors. Eur Rev Med Pharmacol Sci 2010; 14: 249-258.
- GILL S, THOMAS RR, GOLDBERG RM. Review article: colorectal cancer chemotherapy. Aliment Pharmacol Ther 2003; 18: 683-692.
- PARKIN DM, BRAY F, FERLAY J, PISANI P. Global cancer statistics, 2002. CA Cancer J Clin 2005; 55: 74-108.
- Xi ZW, Xin SY, Zhou L, Yuan HX, Wang Q, Chen KX. Downregulation of rho-associated protein kinase 1 by miR-124 in colorectal cancer. World J Gastroenterol 2015; 21: 5454-5464.
- 7) SIEGEL R, NAISHADHAM D, JEMAL A. Cancer statistics, 2013. CA Cancer J Clin 2013; 63: 11-30.
- 8) Thiery JP, Acloque H, Huang RY, Nieto MA. Epithelial-mesenchymal transitions in development and disease. Cell 2009; 139: 871-890.
- 9) ZHANG XF, ZHANG Y, SHEN Z, YANG GG, WANG HD, LI LF, LIU DC, QIU JM. LncRNALUADT1 is overexpressed in colorectal cancer and its expression level is related to clinicopathology. Eur Rev Med Pharmacol Sci 2018; 22: 2282-2286.
- RYAN BM, ROBLES AI, HARRIS CC. Genetic variation in microRNA networks: the implications for cancer research. Nat Rev Cancer 2010; 10: 389-402.
- 11) Wu O, Yang Z, Shi Y, Fan D. MiRNAs in human cancers: the diagnostic and therapeutic implications. Curr Pharm Des 2014; 20: 5336-5347.
- ESQUELA-KERSCHER A, SLACK FJ. Oncomirs, microR-NAs with a role in cancer. Nat Rev Cancer 2006;
 259-260.
- 13) Cal D, Liu Z, Kong G. Molecular and bioinformatics analyses identify 7 circular RNAs involved in

- regulation of oncogenic transformation and cell proliferation in human bladder cancer. Med Sci Monit 2018; 24: 1654-1661.
- 14) Maorano NA, Mallamaci A. The pro-differentiating role of miR-124: indicating the road to become a neuron. RNA Biol 2010; 7: 528-533.
- 15) LI J, SONG Y, WANG Y, Luo J, Yu W. MicroRNA-148a suppresses epithelial-to-mesenchymal transition by targeting ROCK1 in non-small cell lung cancer cells. Mol Cell Biochem 2013; 380: 277-282.
- MEDINA PP, SLACK FJ. MicroRNAs and cancer: an overview. Cell Cycle 2008; 7: 2485-2492.
- 17) HANNAN AJ, KIND PC, BLAKEMORE C. Phospholipase C-beta 1 expression correlates with neuronal differentiation and synaptic plasticity in rat somatosensory cortex. Neuropharmacology 1998; 37: 593-605.
- 18) CABANA-DOMINGUEZ J, RONCERO C, PINEDA-CIRERA L, PALMA-ALVAREZ RF, ROS-CUCURULL E, GRAU-LOPEZ L, ES-OIO A, CASAS M, ARENAS C, RAMOS-QUIROGA JA, RIBASES M, FERNANDEZ-CASTILLO N, CORMAND B. ASSOCIATION of the PLCB1 gene with drug dependence. Sci Rep 2017; 7: 10110.
- 19) Song B, Lin HX, Dong LL, Ma JJ, Jiang ZG. MicroR-NA-338 inhibits proliferation, migration and invasion of gastric cancer cells by the Wnt/β-catenin signaling pathway. Eur Rev Med Pharmacol Sci 2018; 22: 1290-1296.
- 20) LEMIEUX E, CAGNOL S, BEAUDRY K, CARRIER J, RI-VARD N. Oncogenic KRAS signaling promotes the Wnt/β-catenin signaling pathway through LRP6 in colorectal cancer. Oncogene 2015; 34: 4914-4927
- 21) LIVAK KJ, SCHMITTGEN TD. Analysis of relative gene expression data using real-time quantitative PCR and the ^{2-ΔΔ}ct method. Methods 2001; 25: 402-408.
- 22) CHEN WC, KUO TH, TZENG YS, TSAI YC. Baicalin induces apoptosis in SW620 human colorectal carcinoma cells in vitro and suppresses tumor growth in vivo. Molecules 2012; 17: 3844-3857.
- LEI CJ, WANG B, LONG ZX, REN H, PAN QY, LI Y. Investigation of PD-1H in DEN-induced mouse liver cancer model. Eur Rev Med Pharmacol Sci 2018; 22: 5194-5199.
- 24) FRICK VO, RUBIE C, KOLSCH K, WAGNER M, GHADJAR P, GRAEBER S, GLANEMANN M. CCR6/CCL20 chemokine expression profile in distinct colorectal malignancies. Scand J Immunol 2013; 78: 298-305.
- LAKSHMANAN L, MUTHUSAMY K, MARSHAL JJ, KAJAMAIDEEN A, BALTHASAR JJ. In silico insights on tankyrase protein: a potential target for colorectal cancer. J Biomol Struct Dyn 2018; 11: 1-29.
- 26) ALI RM, AL-SHORBAGY MY, HELMY MW, EL-ABHAR HS. Role of Wnt4/β-catenin, Ang II/TGF-beta, NF-kB and IL-18 in attenuating renal ischemia/reperfusion-induced injury in rats treated with Vit D and pioglitazone. Eur J Pharmacol 2018; 831: 68-76.
- 27) Hong L, Han Y, Yang J, Zhang H, Zhao Q, Wu K, Fan D. MicroRNAs in gastrointestinal cancer: prognostic significance and potential role in che-

- moresistance. Expert Opin Biol Ther 2014; 14: 1103-1111.
- 28) Li HG, Zhao LH, Bao XB, Sun PC, Zhai BP. Meta-analysis of the differentiatlly expressed colorectal cancer-related microRNA expression profiles. Eur Rev Med Pharmacol Sci 2014; 18: 2048-2057.
- 29) CHEN Y, LI Y, NIAN Y, LIU D, DAI F, ZHANG J. STAT3 is involved in miR-124-mediated suppressive effects on esophageal cancer cells. BMC Cancer 2015; 15: 306.
- Dong LL, Chen LM, Wang WM, Zhang LM. Decreased expression of microRNA-124 is an independent unfavorable prognostic factor for patients with breast cancer. Diagn Pathol 2015; 10: 45.
- 31) SUN Y, AI X, SHEN S, LU S. NF-kappaB-mediated miR-124 suppresses metastasis of non-smallcell lung cancer by targeting MYO10. Oncotarget 2015; 6: 8244-8254.
- 32) VICINUS B, RUBIE C, FAUST SK, FRICK VO, GHADJAR P, WAGNER M, GRAEBER S, SCHILING MK. miR-21 functionally interacts with 3'UTR of chemokine CCL20 and down-regulates CCL20 expression in miR-21 transfected colorectal cancer cells. Cancer Lett 2012; 316: 105-112.
- 33) BAI W, CHEN Y, YANG J, NIU P, TIAN L, GAO A. Aberrant mRNA profiles associated with chronic benzene poisoning. Exp Mol Pathol 2014; 96: 426-430.
- 34) Li J, Zhao X, Wang D, He W, Zhang S, Cao W, Huang Y, Wang L, Zhou S, Luo K. Up-regulated ex-

- pression of phospholipase C, beta 1 is associated with tumor cell proliferation and poor prognosis in hepatocellular carcinoma. Onco Targets Ther 2016; 9: 1697-1706.
- 35) JI KX, CUI F, QU D, SUN RY, SUN P, CHEN FY, WANG SL, SUN HS. MiR-378 promotes the cell proliferation of non-small cell lung cancer by inhibiting FOXG1. Eur Rev Med Pharmacol Sci 2018; 22: 1011-1019.
- 36) ZHOU L, XU Z, REN X, CHEN K, XIN S. MicroRNA-124 (miR-124) inhibits cell proliferation, metastasis and invasion in colorectal cancer by downregulating Rho-associated protein kinase (ROCK1). Cell Physiol Biochem 2016; 38: 1785-1795.
- 37) ZHANG N, HUANG Y, WU F, ZHAO Y, LI X, SHEN P, YANG L, LUO Y, YANG L, HE G. Codelivery of miR-124 mimic and obatoclax by cholester-ol-penetratin micelles simultaneously induces apoptosis and inhibits autophagic flux in breast cancer in vitro and in vivo. Mol Pharm 2016; 13: 2466-2483.
- 38) YUE Q, ZHANG Y, LI X, HE L, Hu Y, WANG X, XU X, SHEN Y, ZHANG H. MiR-124 suppresses the chemotactic migration of rat mesenchymal stem cells toward HGF by downregulating Wnt/β-catenin signaling. Eur J Cell Biol 2016; 95: 342-353.
- 39) Hu H, WANG G, Li C. miR-124 suppresses proliferation and invasion of nasopharyngeal carcinoma cells through the Wnt/β-catenin signaling by targeting Capn4. Onco Targets Ther 2017; 10: 2711-2720.